Chin. Geogra. Sci. 2019 Vol. 29 No. 2 pp. 192–201
https://doi.org/10.1007/s11769-018-1013-z

Springer Science Press
www.springerlink.com/content/1002-0063

Comparative Study on Coastal Depth Inversion Based on Multi-source Remote Sensing Data

LU Tianqi[1], CHEN Shengbo[1], TU Yuan[2], YU Yan[1], CAO Yijing[1], JIANG Deyang[1]

(1. *College of Geo-exploration Science and Technology*, *Jilin University*, *Changchun* 130026, *China*; 2. *College of Earth Sciences*, *Guilin University of Technology*, *Guilin* 541006, *China*)

Abstract: Coastal depth is an important research focus of coastal waters and is also a key factor in coastal environment. Dongluo Island in South China Sea was taken as a typical study area. The band ratio model was established by using measured points and three multispectral images of Landsat-8, SPOT-6 (Systeme Probatoire d'Observation de la Terre, No.6) and WorldView-2. The band ratio model with the highest accuracy is selected for the depth inversion respectively. The results show that the accuracy of SPOT-6 image is the highest in the inversion of coastal depth. Meanwhile, analyzing the error of inversion from different depth ranges, the accuracy of the inversion is lower in the range of 0–5 m because of the influence of human activities. The inversion accuracy of 5–10 m is the highest, and the inversion error increases with the increase of water depth in the range of 5–20 m for the three kinds of satellite images. There is no linear relationship between the accuracy of remote sensing water depth inversion and spatial resolution of remote sensing data, and it is affected by performance and parameters of sensor. It is necessary to strengthen the research of remote sensor in order to further improve the accuracy of inversion.

Keywords: coastal waters; remote sensing; quantitative inversion; satellite; accuracy comparison

Citation: LU Tianqi, CHEN Shengbo, TU Yuan, YU Yan, CAO Yijing, JIANG Deyang, 2019. Comparative Study on Coastal Depth Inversion Based on Multi-source Remote Sensing Data. *Chinese Geographical Science*, 29(2): 192–201. https://doi.org/10.1007/s11769-018-1013-z

1 Introduction

The coastal waters are defined as waters within 20 nautical miles of the beach, even if the coast is uninhabited or inaccessible (Johnson et al., 2017). Coastal waters are the interface between land and sea and have important ecological value because of their high productivity and system diversity (such as estuaries, coastal wetlands, coral reefs, mangroves, and upwelling areas). It is necessary to investigate the coastal depth, water quality and water temperature, whether it is for reclamation, coastal tourism, shallow sea farming, or shallow sea energy exploration and other activities. Coastal waters have always been the focus of research at home and abroad because of it being most closely related to human activities. Coastal depth is an important research focus of coastal waters and is an important factor in coastal environment (Manessa et al., 2018). The measurement plays an important role in safety of shipping, research of ocean science, simulation of coastal storm surge, construction of coastal facilities, monitoring of marine ecosystem, management of coastal zone, detection of shoreline erosion, and so on (Poupardin et al., 2016).

Bathymetry is mainly measured by shipborne plumb line in earlier times. This kind of operation mode is inefficient, measurement points are sparse, and it is subject to ocean currents. The echo detector based on sonar technology was invented in the 1920s (Li et al., 2016),

Received date: 2017-11-16; accepted date: 2018-03-08

Foundation item: Under the auspices of the Program for Jilin University Science and Technology Innovative Research Team (No. JLUSTIRT, 2017TD-26), Plan for Changbai Mountain Scholars of Jilin Province, China

Corresponding author: CHEN Shengbo. E-mail: chensb@jlu.edu.cn

which marked the entrance of a new era in ocean mapping (Li, 1999; Zhao and Liu, 2008). The sonar sounding system based on the ship is still the main method of coastal bathymetry now. However, it has the shortcoming of time and labor cost and also cannot measure the area where the ship cannot sail. The method of coastal depth measurement based on remote sensing has been developed to make up for the defect of site measurement (Su et al., 2015; Poupardin et al., 2016).

The development of remote sensing technology of water depth can be traced back to the early last century. In the 1930s, the characteristics of water spectrum were researched. Clarke and James (1939) first explored the relationship between absorption coefficient and wavelength of pure water in a wavelength from 0.375 to 0.800 μm. Curcio and Petty (1951) further investigated the relationship between absorption coefficient of 0.700 to 2.500 μm pure water and wavelength. It was found that pure water had the weakest absorption in the blue band near the wavelength of 0.475 μm, and the absorption coefficient tends to increase with the increase of the wavelength. Researchers at the American Environmental Research Institute of Michigan have been working on remote sensing sounding in the late 1960s. They used multi-spectral data such as multispectral scanners, thematic mapper (TM) scanner and aerial photo to study bathymetric model. Lyzenga (1978; 1981) proposed the quantitative analysis method of water depth measurement based on the bottom reflection model. Clark et al. (1987) extracted water depth value from image data of Landsat TM1, TM2 band in the vicinity of Isla de Vieques through the linear multiband method. Mgengel and Spitzer (1991) conducted the multidate mapping of shallow seafloor nearby the Netherlands by using TM image. Bierwirth et al. (1993) assumed that when water quality and sediments are homogeneous, it is possible to extract water depth and information of bottom reflectance using the visible spectrum of TM remote sensing image to build multiband model and applied the model to Shark bay. The result shows that there has a larger error when inversion of deeper water depth by using TM remote sensing image. Sandidge and Holyer (1998) established the artificial neural network model using the correlation between bathymetric information and hyperspectral remote sensing images, and then used the model to invert the depth information of the study area. The data used in the study above is single, and lacking of the comparative study on multi-source remote sensing data.

The research on water depth inversion using multispectral remote sensing data has been rapidly developed (Flener et al., 2012; Abileah, 2013; Eugenio et al., 2015). Three forms of models have been developed, theory interpretation model, semi-theoretical semi-empirical model, and statistical correlation model in the aspect of construction of remote sensing model for water sounding (Jawak et al., 2015). Based on the radiation transfer equation in the water body, the theory interpretation model calculates water depth by measuring the optical parameter inside the water body. Currently, the common theory interpretation model is two-stream approximation model (Lyzenga, 1979; Salama and Verhoef, 2015). Two-stream refers that for any depth Z, water can be divided into two parts: above depth Z and below depth Z; thus, the light radiant flux of water body can be decomposed into upward component and downward component. The radiation flux varies with the water depth can be estimated by studying the value or ratio of upward component and downward component. Due to the participation of water depth variable Z in the analytical process, it is possible to calculate the distribution of water depth using this model. Based on the radiation damping of light in the water, the semi-theoretical semi-empirical model fulfills the remote sensing inversion of water by using the combination of the theoretical model with empirical model, and it can be classified into single-band model (Benny and Dawson, 1983) and multi-bands model (Paredes and Spero, 1983) on account of number of bands to be used. Compared to theoretical interpretation model, semi-theoretical semi-empirical model is simplified by using the combination of the theoretical model with empirical value of research area. Taking advantage of the less required parameters during the calculative process and high accuracy of inversion, it has been widely used in currently remotely sensed bathymetric technology (Su et al., 2008). As one of the widely used research technologies of remotely sensed bathymetric, the statistical correlation model derives water depth data through building the correlativity between radiance of remote sensing image and measured water depth (Lyzenga, 1978; 1981; Figueiredo et al., 2016). As compared to the theoretical interpretation model and semi-theoretical semi-empirical model, statistical correlation model does not require optical parameters on the inner water body, and the simple calcu-

lation makes it widely used. Nevertheless, due to the unique specific area of water in research, the factual correlation of measured water depth and radiance of remote sensing image cannot be guaranteed, thus leading to an undesirable result (Su et al., 2014).

Not only is the implementation of the model a key factor to improve the accuracy of water depth inversion but also the quantity of remote sensing data can affect it. However, the previous research concentrated on comparing the accuracy of different inverse methods, paying less attention on analyzing error of different remote sensing data used for inverse water depth.

The sea area of Dongluo Island is located in the South China Sea. Taking the sea area of Dongluo Island as an example, we established the band ratio models using three multispectral images of Landsat-8, SPOT-6 (Systeme Probatoire d'Observation de la Terre, No.6), WorldView-2 and measured points. The band ratio model with the highest accuracy was selected for the depth inversion. This study compares accuracy of inversion of remote sensing data that were acquired by three different sensors, and analyzes the inversion accuracy of three remote sensing data in the range of water depths of 0–5, 5–10, 10–15 and 15–20 m. On this basis, the remote sensing image with the highest accuracy of the water depth inversion is evaluated. This provides reference for the selection of remote sensing data for coastal water depth inversion.

2 Materials and Methods

2.1 Study area

Dongluo Island seas, located in the north of South China Sea (Fig. 1), have geographical coordinates between 108°59′05.78″E and 109°06′47.94″E and between 18°16′09.15″N and 18°22′54.30″N. They belong to Hainan Province, China, and experience tropical monsoon climate at low latitudes. The seawater in this area has strong penetrability and the maximum depth is about 20 m.

2.2 Model principles

The spectral characteristics of the objects reflect their own attributes and status, so different objects have different spectral characteristics. The optical characteristics of water are determined by absorption and scattering properties of the optical active substance. The spectral proprieties of water derived by using remote sensing system to measure radiance of a range of wavelengths are the basics of inversion of water depth using remote sensing.

The material compositions decide the spectral signature of water; it can also be affected by the statue of water. After a series of reflection and absorption of water, the radiance of sunlight reaching the sensor can be divided into three parts: 1) the solar radiance scattered

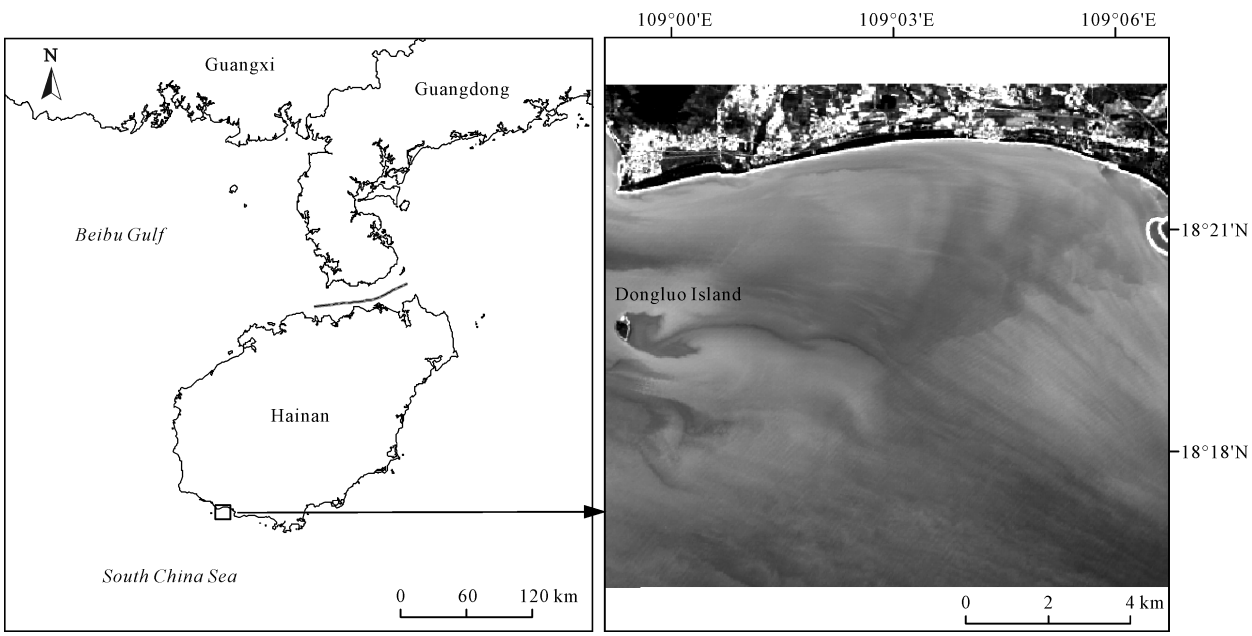

Fig. 1 Location of study area

by the atmosphere reaches the sensor; 2) the solar radiance reflected by water reaches the sensor; 3) the backward scattered light of water and reflected light of underwater returns to the atmosphere and is intercepted by the sensor. This part is called water-leaving radiance which includes the information of water (Fig. 2). The reflectance of a range of wavelength usually has significant differences due to the water depth, which is the theoretical basis of quantitative inversion of water depth of remote sensing.

Band ratio model is developed on the basis of the single-band and dual-band models. It builds the linear or nonlinear statistical relation models between remote sensing data and synchronous measured depth based on the decay properties of light in water. This model combines the intrinsic optical quantum and preventative optical quantum of water according to the radiation transfer theory (Li et al., 2008). Using some assumption conditions to reduce the spatiotemporal differences of the unit intrinsic optical mass to invert the parameters of water, we simplify the model with approximate relationship, reducing the unknown value and interdependent relationship. Therefore, the band ratio model has certain physical significance and high inversion accuracy, thus can be used widely.

According to Bouguer theorem (Lyzenga, 1978), the changes of light radiation flux as water depth fulfill exponential decay (Huang et al., 2017), namely:

$$I(Z) = I_0 e^{-KZ} \tag{1}$$

In the formula, I_0 and $I(Z)$ represent the light on the water surface and radiation flux of the water depth Z, respectively. K represents decay degree. Thus, we can obtain the simple model (Lyzenga, 1978; Clark et al., 1987):

$$R_{\mathrm{E}} = \alpha R_{\mathrm{b}} \mathrm{e}^{-2KZ} + R_{\mathrm{W}} \tag{2}$$

In the formula, R_{E} is the reflection received by sensor; K is the decay coefficient of water; R_{W} is the reflectance of water; R_{b} is the reflectance of underwater; α is a comprehensive factor, which delivers the effects of solar radiance transmission in the water surface and atmosphere; and sunlight reflects on the water surface.

According to the equation above:

$$R_{\mathrm{E}} - R_{\mathrm{W}} = \alpha R_{\mathrm{b}} \mathrm{e}^{-2KZ} \tag{3}$$

Through ratio operation on the bands 1 and 2, we can derive:

$$\frac{R_{\mathrm{E1}} - R_{\mathrm{W1}}}{R_{\mathrm{E2}} - R_{\mathrm{W2}}} = \frac{R_{\mathrm{b1}}}{R_{\mathrm{b2}}} e^{-2(K_1 - K_2)Z} \tag{4}$$

Further, it can be derived that:

$$Z = -\frac{1}{2(K_1 - K_2)} \ln \frac{R_{\mathrm{E1}} - R_{\mathrm{W1}}}{R_{\mathrm{E2}} - R_{\mathrm{W2}}} + \frac{1}{2(K_1 - K_2)} \ln \frac{R_{\mathrm{b1}}}{R_{\mathrm{b2}}} \tag{5}$$

Assuming bands 1 and 2 keep constant reflectances on different substrates, $\frac{R_{\mathrm{b1}}}{R_{\mathrm{b2}}}$ is a constant. The difference in value of the decay coefficient of the two bands in the different types of water does not change.

In Equation (5):

$$a = \frac{1}{2(K_1 - K_2)}, c = \frac{1}{2(K_1 - K_2)} \ln \frac{R_{\mathrm{b1}}}{R_{\mathrm{b2}}}, X_i = R_{\mathrm{E}i} - R_{\mathrm{W}i},$$

$i = 1$ or 2

Then, Eq. (5) can be simplified as:

$$Z = a \ln \left(\frac{X_1}{X_2} \right) + c \tag{6}$$

Equation (6) is the band ratio model expression (Clark et al., 1987; Lu et al., 2016).

To some extent, the band ratio model eliminates the attenuation coefficient due to uneven water body and the effect of different reflectances in the bottom due to the differences of sediments. In addition, the band ratio model can also impair the sun elevation angle, surface wave, and satellite attitude; the scan angle changes such difference effects on the version of water depth.

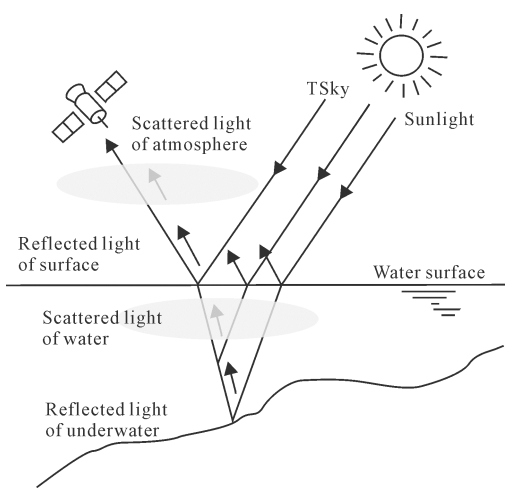

Fig. 2 Schemata of optical dissemination in water

The mean relative error (MRE) was selected to measure the accuracy of the depth inversion. It is the average of the absolute values of the sample relative error:

$$\bar{E} = \frac{1}{n}\sum_{i}^{n} |e_i| = \frac{1}{n}\sum_{i}^{n} \left| \frac{\hat{x}_i - x_i}{x_i} \times 100\% \right| \quad (7)$$

where $\bar{E}$ is mean relative error, n is sample size, $\hat{x}_i$ is water depth of inversion, x_i is measured water depth, and e_i is relative error.

2.3 Data and preprocessing

The study used three types of data, including the United States (US) Landsat-8, the French SPOT-6 and the US WorldView-2 satellite data. The acquisition time, spectral values of the used band, and spatial resolution are listed in Table 1. Water depth-measured data used the single-point sonar data measured by Guangzhou Marine Geological Survey in November 2014. There are multiple measured points in the same pixel due to the fact that the sounding points of the survey line are dense, which will cause the measured points at different depths of the pixel correspond to the digital number (DN) value of the same pixel and result in an increase in inversion error. Therefore, the number of sounding points becomes less in order to avoid increasing the inversion error. The distribution of measured points is shown in Fig. 3. Adopted satellite remote sensing data are applied in the fourth quarter of 2013. It can be applied because the image time is close to the measured data collection time.

Generally, the remote sensing digital image shows the pixel DN value which is the dimensionless value. Using the DN value can only compare the same-scene image. Only by converting the image DN value into the radiation luminance value of the corresponding pixel

Table 1 Remote sensing satellite parameters of different sensors

Parameters	Landsat-8	SPOT-6	WorldView-2
Acquisition time	2013-10-16	2013-12-07	2013-10-07
Spectral value (μm)	Blue: 0.483; Green: 0.561; Red: 0.655; NIR: 0.865	Blue: 0.485; Green: 0.560; Red: 0.660; NIR: 0.825	Blue: 0.480; Green: 0.545; Red: 0.660; NIR: 0.833
Spatial resolution (m)	30.0	6.0	1.8

Notes: SPOT-6 is the Systeme Probatoire d'Observation de la Terre, No.6. NIR is the band of near infrared

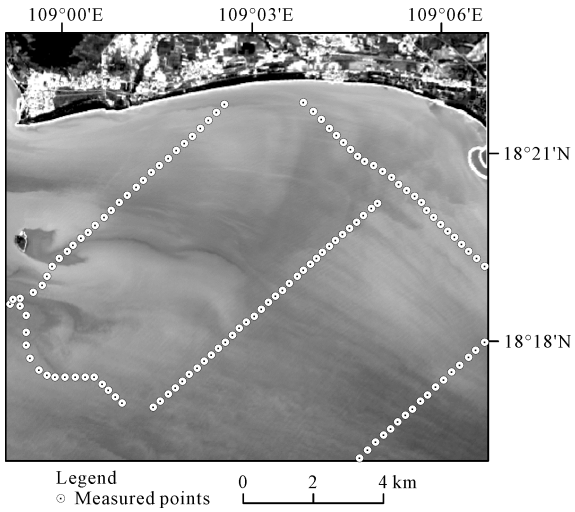

Fig. 3 Measured points distribution of study area

can the remote sensing data obtained from different locations, at different times, and from different types of sensors be quantitatively compared and applied to meet the needs of the research. The process of conversion is called radiometric calibration.

The geometric distortion of the original image is very large because it is affected by the sensor platform latitude, height, and speed changes and by various factors such as panoramic distortion, Earth curvature, and the instantaneous field of view with a nonlinear characteristic of the sensor in the scanning, which has brought difficulties to the quantitative analysis. Therefore, the images must be corrected in order to use remote sensing images for analysis and research work. Remote sensing data still need to do further geometric corrections after correction in the receiving sector. In the study, the geometric correction of the remote sensing image is carried out by using the ground control point. Selecting the corresponding points as the control points to establish the correspondence between the distortion space and the correction space, all the pixels of the distortion space are transformed into the correction space, and the geometric correction of the remote sensing image is carried out by the correspondence between the two sets of coordinates.

The purpose of remote sensing is using sensors to efficiently collect electromagnetic radiation from the ground. However, the measured value of the remote sensing sensor is not the same as the actual spectral emissivity of the object due to the transmission of electromagnetic waves affected by the remote sensing sensor sensitivity analysis, the conditions of light condi-

tions, and the role of human impact in the atmosphere and the sensor in the measurement process, so it is radiation distortion in the measured value. Atmospheric correction is the process of converting radiance into the surface reflectance, the main purpose of which is to eliminate the effects of atmospheric scattering on radiation distortion.

Fast Line of Sight Atmospheric Analysis of Spectral Hypercube (FLAASH) is an atmospheric correction model of high spectral radiant energy image reflectance inversion, which can accurately compensate for atmospheric effects. The applicable wavelength range includes visible-to-near infrared and short-wave infrared. In the study, atmospheric correction module FLAASH in the Environment for Visualizing Images was used to realize the atmospheric correction of the image.

It can be seen from Fig. 4 that the image after atmospheric correction has a significant absorption peak and a significant reflection peak in the visible light of 0.43–0.70 μm. Specifically, the absorption peak near 0.47 μm is mainly due to the presence of chlorophyll a in water (Gitelson, 1992), while the reflection peak near 0.56 μm is due to the weak absorption of chlorophyll and carotene and the scattering effect of cells in water (Gordon, 1979; Shu et al., 2000). The characteristics above indicate that the image basically removes the influence of the factors such as water vapor particles in the air, and the spectral curve of the water body tends to be normal.

3 Results

The highest correlation coefficient of different band ratio models for Landsat-8, SPOT-6 and WorldView-2 is selected as the depth inversion model. On this basis, the inversion accuracy of the three data in different depth ranges is analyzed.

3.1 Model comparison based on different band ratios

The reflectance values of the pixels that corresponding to the measured points shown in Fig. 3 at each band were extracted.

In this study, we build six band ratio models with blue, green, red, and near-infrared bands. The parameters of the band ratio model are regression analyzed by using the attribute information of measured points of the water depth which includes the reflectance value and water depth of each band of the image. Correlation coefficient is shown in Table 2. It can be seen from table that the correlation coefficient of blue-near-infrared band ratio model of Landsat-8 image is the highest, and R^2 is equal to 0.5073; the correlation coefficient of green-red band ratio model of SPOT-6 is the highest, and R^2 is equal to 0.7064; the correlation coefficient of blue-green band ratio model of WorldView-2 is the highest, and R^2 is equal to 0.6679 (Fig. 5). Thus, we choose the above models as the final models to inverse the water depth.

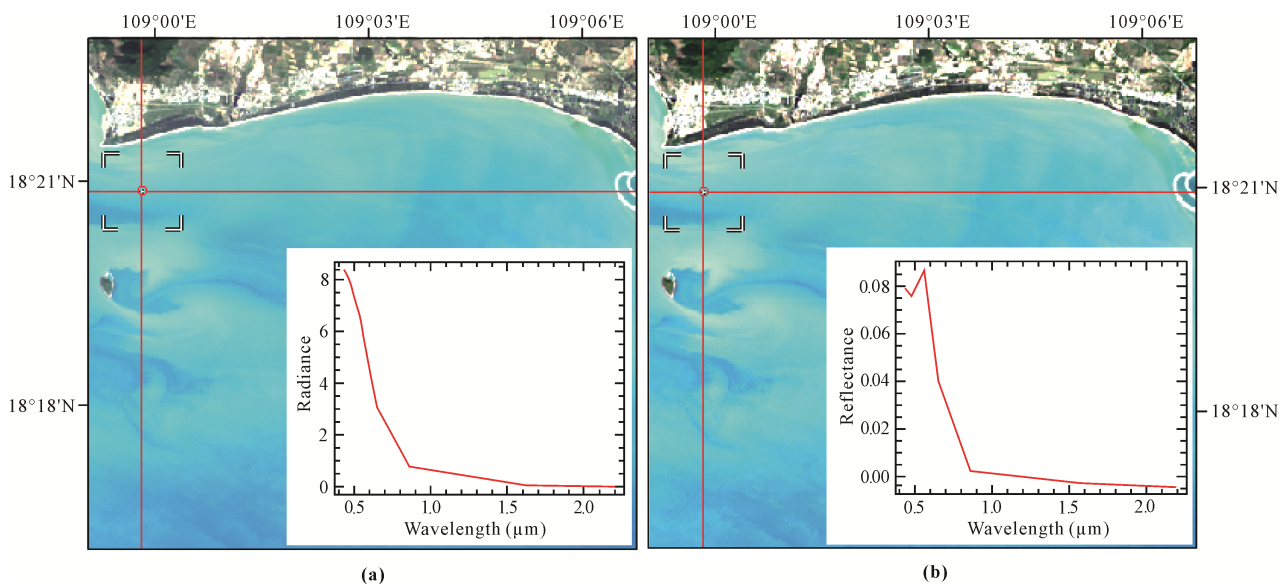

Fig. 4 Comparison of Landsat-8 spectra before and after atmospheric correction. (a): Image of radiance before atmospheric correction; (b): Image of reflectance after atmospheric correction

Table 2 Correlation coefficient of different band ratio models for different satellites

Satellite	B/G	B/R	B/NIR	G/R	G/NIR	R/NIR
Landsat-8	0.1698	0.0063	0.5073	0.0259	0.3163	0.2935
SPOT-6	0.2656	0.6528	0.3201	0.7064	0.2221	0.7008
WorldView-2	0.6679	0.3059	0.0110	0.0258	0.1261	0.2505

Notes: B, G, R are the abbreviation for the band of blue, green and red, respectively. NIR is the band of near infrared

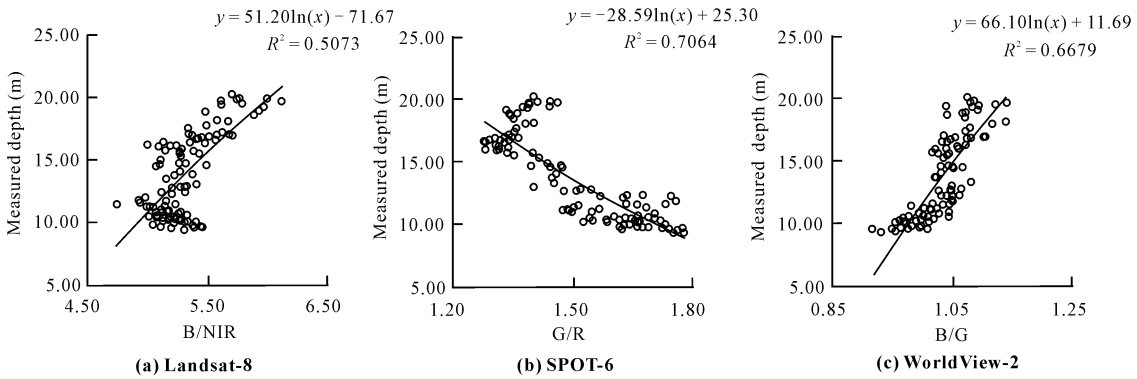

Fig. 5 Scatter plots of band ratio and measured depth for Landsat-8, SPOT-6 and WorldView-2. B, NIR, G, R are the abbreviation for the band of blue, near infrared, green and red, respectively. SPOT-6, remote sensing satellite, is the abbreviation for the French for Systeme Probatoire d'Observation de la Terre, No.6

3.2 Accuracy analysis of depth inversion

Putting the regression parameter derived from band ratio and values of corresponding water depth points into corresponding band ratio model, the inversion result is shown in Fig. 6.

It can be seen that the inversion results of three different sensors overall have good consistency. The water depths in the 'A' box in Fig. 6 are deeper, and they are smaller in the 'B' box. The trend of water depth is consistent along the direction of curve 'C' for three satellite data. It is verified that the reliability of water depth inversion results from another aspect.

Calculating mean relative error of water depth inversion from remote sensing image in different depth ranges, the results are shown in Table 3.

Mean relative errors of inversion water depth results are analyzed. The inversion errors of SPOT-6 image are the least in three ranges of water depths, 0–5, 5–10 and 10–15 m, respectively, 30.99%, 13.62%, and 21.68%. The inversion error in 0–5 m is bigger because of the location of this area; it lies in the zone of wave breaking, where wave can increase the sediment in the water. This affects the reflection of light on the water surface and the scattering in the water and leads to the increase the inversion error. The inversion error of the Landsat-8 image is the least (32.5%) in the range of 15–20 m water depth.

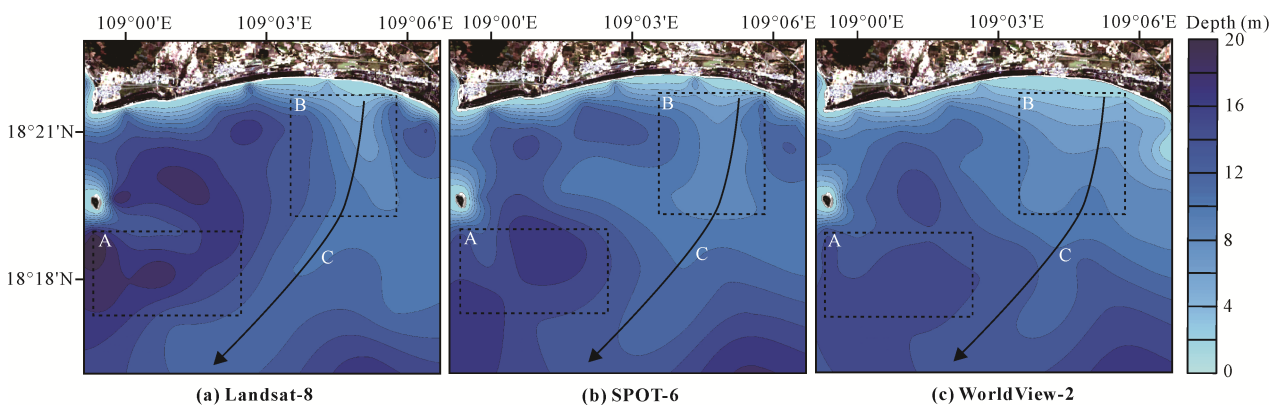

Fig. 6 Depth inversion results of Landsat-8, SPOT-6 and WorldView-2

Table 3 Mean relative error of depth inversion and measured depth (%)

Depth range (m)	Landsat-8	SPOT-6	WorldView-2
0–5	40.89	30.99	31.28
5–10	22.72	13.62	22.31
10–15	23.12	21.68	24.35
15–20	32.50	33.65	33.22
Average	29.81	24.89	27.54

It can be seen from Fig. 7 that the order of errors of the inversion water depth array from small to large are SPOT-6, WorldView-2 and Landsat-8 in the range of 0–5 and 5–10 m. However, the order changes in the range of 10–15 m. The inversion error of SPOT-6 image is still the least, but the inversion error of WorldView-2 is a little bigger than the inversion error of Landsat-8. When the water depth is greater than 15 m, the inversion relative error of Landsat-8 is the least, followed by WorldView-2, and the inversion relative error of SPOT-6 is the most.

4 Discussion

The remote sensing technology of water depth developed rapidly. The nature of remote sensor has an important influence on the inversion accuracy of water depth. In order to improve the accuracy of remote sensing inversion further, the research of remote sensor must be strengthened.

As the important collector of water depth information in remote sensing inversion of water depth, the remote sensor noise has an important influence on the accuracy of inversion (Jay et al, 2017). The data obtained by different sensors have their own characteristics in spectral resolution and spatial resolution (Lee et al., 2012; Odermatt et al., 2012). Therefore, the results of water depth information show some differences. The final effective information of the depth information received by the remote sensor is to highlight the depth information in water depth remote sensing. The chlorophyll, suspended sediment, chromophoric dissolved organic matter, and other information of the water body as the noise in water depth remote sensing must be suppressed or removed, so requirements for the spectral resolution of remote sensor are put forward. The experiences show that the image of SPOT-6 has the high accuracy in the range of 0–15 m water depths. The main reasons are analyzed, the remote sensor of SPOT-6 has high stability and signal-to-noise because of SPOT-6 is a mature commercial satellite; the remote sensor can suppress the noise and highlight the useful information in water because of the high spectral resolution. Meanwhile, the accuracy of the inversion has reached the highest in the range of 5–10 m (Lu et al., 2016), in particular, the mean relative error of SPOT-6 reached 13.62%. The reason for this is that the water surface in the range of 5–10 m is relatively stable and has a certain distance from coast. These make the water quality better, so the water body can be completely penetrated by the remote sensor (Di et al., 1999). The technology of water depth remote sensing is an important auxiliary means for conventional bathymetry. The scope of engineering survey and the precision of the mapping are also certain requirements for the spatial resolution of remote sensor. In the future of the inversion of remote sensing, improving the system stability and signal-to-noise ratio of the remote sensor, using the hyperspectral remote sensing data to highlight the depth information, and the combination of remote sensing data with different spectral resolution and spatial resolution, which will be of significance to improve the accuracy of remote sensing inversion, is necessary.

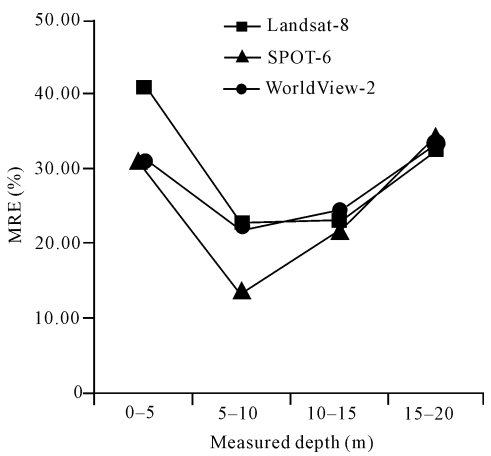

Fig. 7 Mean relative error (MRE) of depth inversion results for different satellites in different measured depth ranges.

In conclusion, the remote sensing of water depth has the advantages of being macroscopic, dynamic and objective. It has played a certain role in practical engineering and has a wide application prospect as one of the emerging technologies in the field of remote sensing and is an important complement to conventional water depth measurements. It is necessary to strengthen the

research of remote sensor, the mechanism of water depth remote sensing, and the construction of model in future research (Li et al., 2016). The remote sensing spectral range and the band combination are scientifically selected to highlight the water depth information, and the influence of the water body and the material of the atmosphere on the water depth information are taken into account to further improve the accuracy and application range of the remote sensing inversion.

5 Conclusions

In terms of the depth of coastal waters in tropical regions, this study selected three different kinds of sensors to find out the inverse water depth of remote sensing image, and the results showed that the highest accuracy of water depth inversion is SPOT-6 image. The least accuracy of water depth inversion is in the range of 0–5 m due to the effects of human activities offshore, which has a big decay coefficient; in addition, this area belongs to ocean crushed zone, thus surface roughness of the ocean is big and measurable depth is small. On the one hand, the accuracy of water depth inversion is highest in the range of 5–10 m, the error of inversion turns to progressive tendency with the increase of depth, which means that there is a negative correlation between water depth and inverse accuracy. On the other hand, there is no linear relationship between the accuracy of remote sensing water depth inversion and spatial resolution of remote sensing data, and it is affected by performance and parameters of sensor. Therefore, it is necessary to strengthen the research of remote sensor in order to further improve the accuracy of inversion. In addition, many other factors such as suspended particle, yellow substance, and chlorophyll concentration also affect the accuracy of inversion. This study did not consider the above factors, which is the direction of follow-up research.

Acknowledgment

We would like to thank Guangzhou Marine Geological Survey of China for its data support.

References

Abileah R, 2013. Mapping near shore bathymetry using wave kinematics in a time series of WorldView-2 satellite images. *Proceesings of 2013 IEEE International Geoscience and Remote Sensing Symposium (IGARSS)*. Melbourne, VIC: IEEE, 2274–2277. doi: 10.1109/IGARSS.2013.6723271

Benny A H, Dawson G J, 1983. Satellite imagery as an aid to bathymetric charting in the Red Sea. *The Cartographic Journal*, 20(1): 5–16. doi: 10.1179/caj.1983.20.1.5

Bierwirth P N, Lee T J, Burne R V, 1993. Shallow sea-floor reflectance and water depth derived by unmixing multispectral imagery. *Photogrammetric Engineering and Remote Sensing*, 59(3): 331–338.

Clark R K, Fay T H, Walker C L, 1987. *A comparison of models for remotely sensed bathymetry*. MS, USA: Naval Ocean Research and Development Activity Stennis Space Center, AD–A197973.

Clarke G L, James H R, 1939. Laboratory analysis of the selective absorption of light by sea water. *Journal of the Optical Society of America*, 29(2): 43–55. doi: 10.1364/JOSA.29.000043

Curcio J A, Petty C C, 1951. The near infrared absorption spectrum of liquid water. *Journal of the Optical Society of America*, 41(5): 302–304. doi: 10.1364/JOSA.41.000302

Di Kaichang, Ding Qian, Chen Wei et al., 1999. Shallow water depth extraction and chart production from TM images in Nansha Islands and nearby sea area. *Remote Sensing for Land and Resources*, 3: 59–64. (in Chinese)

Eugenio F, Marcello J, Martin J, 2015. High-resolution maps of bathymetry and benthic habitats in shallow-water environments using multispectral remote sensing imagery. *IEEE Transactions on Geoscience and Remote Sensing*, 53(7): 3539–3549. doi: 10.1109/TGRS.2014.2377300

Figueiredo I N, Pinto L, Gonçalves G, 2016. A modified Lyzenga's model for multispectral bathymetry using Tikhonov regularization. *IEEE Geoscience and Remote Sensing Letters*, 13(1): 53–57. doi: 10.1109/LGRS.2015.2496401

Flener C, Lotsari E, Alho P et al., 2012. Comparison of empirical and theoretical remote sensing based bathymetry models in river environments. *River Research and Applications*, 28(1): 118–133. doi: 10.1002/rra.1441

Gitelson A, 1992. The peak near 700 nm on radiance spectra of algae and water: relationships of its magnitude and position with chlorophyll concentration. *International Journal of Remote Sensing*, 13(17): 3367–3373. doi: 10.1080/01431169208904125

Gordon H R, 1979. Diffuse reflectance of the ocean: the theory of its augmentation by chlorophyll a fluorescence at 685 nm. *Applied Optics*, 18(8): 1161–1166. doi: 10.1364/AO.18.001161

Huang R Y, Yu K F, Wang Y H et al., 2017. Bathymetry of the coral reefs of Weizhou Island based on multispectral satellite images. *Remote Sensing*, 9(7): 750. doi: 10.3390/rs9070750

Jawak S D, Vadlamani S S, Luis A J, 2015. A synoptic review on deriving bathymetry information using remote sensing technologies: models, methods and comparisons. *Advances in Remote Sensing*, 4(2): 57480. doi: 10.4236/ars.2015.42013

Jay S, Guillaume M, Minghelli A et al., 2017. Hyperspectral remote sensing of shallow waters: considering environmental

noise and bottom intra-class variability for modeling and inversion of water reflectance. *Remote Sensing of Environment*, 200: 352–367. doi: 10.1016/j.rse.2017.08.020

Johnson S Y, Cochrane G R, Golden N E et al., 2017. The California seafloor and coastal mapping program: providing science and geospatial data for California′s State waters. *Ocean and Coastal Management*, 140: 88–104. doi: 10.1016/j. ocecoaman.2017.02.004

Lee Z, Hu C, Arnone R et al., 2012. Impact of sub-pixel variations on ocean color remote sensing products. *Optics Express*, 20(19): 20844–20854. doi: 10.1364/OE.20.020844

Li Jiabiao, 1999. *Principles, Technology and Methods of Multibeam Survey*. Beijing: China Ocean Press. (in Chinese)

Li J R, Zhang H G, Hou P F et al., 2016. Mapping the bathymetry of shallow coastal water using single-frame fine-resolution optical remote sensing imagery. *Acta Oceanologica Sinica*, 35(1): 60–66. doi: 10.1007/s13131-016-0797-x

Li Qingquan, Lu Yi, Hu Shuibo et al., 2016. Review of remotely sensed geo-environmental monitoring of coastal zones. *Journal of Remote Sensing*, 20(5): 1216–1229. (in Chinese)

Li Xian, Chen Shengbo, Wang Xuhui et al., 2008. Study based on radioactive transfer model of the quantitative remote sensing of water bottom reflectance. *Journal of Jilin University* (*Earth Science Edition*), 38(S1): 235–237. (in Chinese)

Lu Tianqi, Chen Shengbo, Guo Tiantian et al., 2016. Offshore bathymetry retrieval from SPOT-6 image. *Journal of Marine Sciences*, 34(3): 51–56. (in Chinese)

Lyzenga D R, 1978. Passive remote sensing techniques for mapping water depth and bottom features. *Applied Optics*, 17(3): 379–383. doi: 10.1364/AO.17.000379

Lyzenga D R, 1979. Shallow-water reflectance modeling with applications to remote sensing of the ocean floor. *Proceedings of the 13th International Symposium on Remote Sensing of Environment*. Ann Arbor, Michigan: Environmental Research Institute of Michigan, 583–602.

Lyzenga D R, 1981. Remote sensing of bottom reflectance and water attenuation parameters in shallow water using aircraft and Landsat data. *International Journal of Remote Sensing*, 2(1): 71–82. doi: 10.1080/01431168108948342

Manessa M D M, Kanno A, Sagawa T et al., 2018. Simulation-based investigation of the generality of Lyzenga′s multispectral bathymetry formula in Case-1 coral reef water. *Estuarine, Coastal and Shelf Science*, 200: 81–90. doi: 10.1016/j.ecss.2017.10.014

Mgengel V, Spitzer R J, 1991. Application of remote sensing data to mapping of shallow sea-floor near by Netherlands. *International Journal of Remote Sensing*, 57(5): 473–479.

Odermatt D, Gitelson A, Brando V E et al., 2012. Review of constituent retrieval in optically deep and complex waters from satellite imagery. *Remote Sensing of Environment*, 118: 116–126. doi: 10.1016/j.rse.2011.11.013

Paredes J M, Spero R E, 1983. Water depth mapping from passive remote sensing data under a generalized ratio assumption. *Applied Optics*, 22(8): 1134–1135. doi: 10.1364/AO.22.001134

Poupardin A, Idier D, de Michele M D et al., 2016. Water depth inversion from a single SPOT-5 dataset. *IEEE Transactions on Geoscience and Remote Sensing*, 54(4): 2329–2342, doi: 10.1109/TGRS.2015.2499379

Salama M S, Verhoef W, 2015. Two-stream remote sensing model for water quality mapping: 2SeaColor. *Remote Sensing of Environment*, 157: 111–122. doi: 10.1016/j.rse.2014.07.022

Sandidge J C, Holyer R J, 1998. Coastal bathymetry from hyperspectral observations of water radiance. *Remote Sensing of Environment*, 65(3): 341–352. doi: 10.1016/S0034-4257(98)00043-1

Shu Xiaozhou, Yin Qiu, Kuang Dingbo, 2000. Relationship between algal chlorophyll concentration and spectral reflectance of inland water. *Journal of Remote Sensing*, 4(1): 41–45. (in Chinese)

Su H B, Liu H X, Heyman W D, 2008. Automated derivation of bathymetric information from multi-spectral satellite imagery using a non-linear inversion model. *Marine Geodesy*, 31(4): 281–298. doi: 10.1080/01490410802466652

Su H B, Liu H X, Wang L et al., 2014. Geographically adaptive inversion model for improving bathymetric retrieval from satellite multispectral imagery. *IEEE Transactions on Geoscience and Remote Sensing*, 52(1): 465–476. doi: 10.1109/TGRS.2013.2241772

Su H B, Liu H X, Wu Q S, 2015. Prediction of water depth from multispectral satellite imagery—the regression Kriging alternative. *IEEE Geoscience and Remote Sensing Letters*, 12(12): 2511–2515. doi: 10.1109/LGRS.2015.2489678

Zhao Jianhu, Liu Jingnan, 2008. *Multi-beam Sounding Technology and Image Data Processing*. Wuhan: Wuhan University Press. (in Chinese)